

value E_{η_1} was taken as $-0.51 \text{ kcal}\cdot\text{mol}^{-1}$. This energy value of η_1 is almost the same as that proposed by Abe, which is $-0.64 \text{ kcal}\cdot\text{mol}^{-1}$. The difference between E_{η_1} for the oligomers and that for 2,4-dimethoxypentane suggests that interaction farther than three bonds influences the first-order interaction η_1 .

Gauche Effect

For molecules containing electronegative atoms the semiempirical energy calculation does not agree with experimental data. However, by taking into consideration the gauche effect, the estimated conformational characters become consistent with those observed. The gauche effect has been noted for the atom pairs in gauche situations such as $\text{O}\cdots\text{O}$, $\text{O}\cdots\text{C}$, and $\text{F}\cdots\text{F}$.³¹ The energies of the gauche effects are in the range of ca. $0\text{--}1 \text{ kcal}\cdot\text{mol}^{-1}$ but they cannot be determined only by the species of the atoms in the gauche arrangement. Abe¹³ proposed the gauche effect for E_{η} to be $-0.2 \text{ kcal}\cdot\text{mol}^{-1}$ from experimental data, that is, coupling constants of 2,4-dimethoxypentane, the dipole moment, and the characteristic ratio of polymers. Our investigation results in a value of $-0.56 \text{ kcal}\cdot\text{mol}^{-1}$ for the gauche effect, which is a little larger than the value proposed by Abe. One of the causes of this difference seems to be that the energy E_{η_1} for the \bar{G} form estimated by Abe is higher than our results. The gauche effect, which is derived from the incompleteness of the functions for the conformational energy calculation, is not the extra stabilization effect of the gauche arrangement. Therefore, the energy functions as used here should be modified by the experimental results, as described in this paper.

Registry No. Ia, 10138-89-3; Ib, 5870-82-6; Ic, 85883-21-2; (\pm)-(R*,R*)-IIa, 85883-17-6; (\pm)-(R*,R*)-IIb, 85883-19-8; (\pm)-(R*,R*)-IIc, 85883-22-3; (\pm)-(R*,S*)-IIIa, 85883-18-7; (\pm)-(R*,S*)-IIIb, 85883-20-1; (\pm)-(R*,S*)-IIIc, 85883-23-4; 2,4-dimethoxypentane, 41021-50-5.

References and Notes

- Flory, P. J. "Statistical Mechanics of Chain Molecules"; Intersciences: New York, 1969.
- Abe, A.; Jernigan, R. L.; Flory, P. J. *J. Am. Chem. Soc.* **1966**, *88*, 631.
- Moritani, T.; Fujiwara, Y. *J. Chem. Phys.* **1973**, *59*, 1175.
- Fujiwara, Y.; Flory, P. J. *Macromolecules* **1970**, *3*, 43.
- Matsuzaki, K.; Sakota, K.; Okada, M. *J. Polym. Sci., Part A-2* **1969**, *7*, 1444.
- Natta, G.; Bassi, I. W.; Corradini, P. *Makromol. Chem.* **1956**, *18/19*, 455.
- Bassi, I. W. *Atti Accad. Naz. Lincei, Cl. Sci. Fis., Mat. Nat., Rend.* **1960**, *29* (8), 193.
- Takeda, M.; Imamura, Y.; Okamura, S.; Higashimura, T. *J. Chem. Phys.* **1960**, *33*, 631.
- Pohl, H. A.; Zabusky, H. H. *J. Phys. Chem.* **1962**, *66*, 1390.
- Luisi, P. L.; Chiellini, E.; Franchini, P. F.; Orienti, M. *Makromol. Chem.* **1968**, *112*, 197.
- Pino, P.; Luisi, P. L. *J. Chim. Phys. Phys.-Chim. Biol.* **1968**, *65*, 130.
- Manson, J. A.; Arquette, G. J. *Makromol. Chem.* **1960**, *37*, 187.
- Abe, A. *Macromolecules* **1977**, *10*, 34.
- Bak, K.; Elefante, G.; Mark, J. E. *J. Phys. Chem.* **1967**, *71*, 4007.
- Abe, A.; Mark, J. E. *J. Am. Chem. Soc.* **1976**, *98*, 6468.
- Mark, J. E.; Flory, P. J. *J. Am. Chem. Soc.* **1965**, *87*, 1415.
- Abe, A.; Hirano, T.; Tsuruta, T. *Macromolecules* **1979**, *12*, 1092.
- Abe, A.; Hirano, T.; Tsuji, K.; Tsuruta, T. *Macromolecules* **1979**, *12*, 1100.
- Hirano, T.; Miyajima, T. *Polym. Prepn. Jpn.* **1981**, *30*, 1858.
- Bovey, F. A.; Tiers, G. V. D. *J. Polym. Sci.* **1960**, *44*, 173.
- Ramey, K. C.; Field, N. D.; Hasegawa, I. *J. Polym. Sci., Part B* **1964**, *2*, 865.
- Dombroski, J. R.; Sarko, A.; Scheurch, C. *Macromolecules* **1971**, *4*, 93.
- Matsuzaki, K.; Ito, H.; Kawamura, T.; Uryu, T. *J. Polym. Sci., Polym. Chem. Ed.* **1973**, *11*, 971.
- Matsuzaki, K.; Sakota, K. *Makromol. Chem.* **1971**, *143*, 115.
- Hatada, K.; Hasegawa, T.; Kitayama, T.; Yuki, H. *J. Polym. Sci., Polym. Lett. Ed.* **1976**, *14*, 395.
- Higashimura, T.; Hirokawa, Y.; Matsuzaki, K.; Uryu, T. *J. Polym. Sci., Polym. Chem. Ed.* **1980**, *18*, 1489.
- Matsuzaki, K.; Morii, H.; Inoue, N.; Kanai, T.; Higashimura, T. *Makromol. Chem.* **1981**, *182*, 2421.
- Cesari, M.; Perego, G.; Marconi, W. *Makromol. Chem.* **1966**, *94*, 194.
- Blukis, U.; Kasai, P. H.; Myers, R. J. *J. Chem. Phys.* **1963**, *38*, 2753.
- Matsuzaki, K.; Morii, H.; Kanai, T.; Fujiwara, Y. *Macromolecules* **1981**, *14*, 1004.
- Hirota, E. *J. Chem. Phys.* **1962**, *37*, 283.
- Mark, J. E.; Flory, P. J. *J. Am. Chem. Soc.* **1965**, *87*, 1415.
- Mark, J. E.; Flory, P. J. *J. Am. Chem. Soc.* **1966**, *88*, 3702.
- Mark, J. E. *J. Am. Chem. Soc.* **1966**, *88*, 3708.
- Mark, J. E. *J. Polym. Sci., Part B* **1966**, *4*, 825.
- Morii, H.; Fujishige, S.; Matsuzaki, K.; Uryu, T. *Makromol. Chem.* **1982**, *183*, 1445.

Excluded Volume in Star Polymers: Chain Conformation Space Renormalization Group

Akira Miyake[†] and Karl F. Freed*

The James Franck Institute and the Department of Chemistry, The University of Chicago, Chicago, Illinois 60637. Received December 13, 1982

ABSTRACT: The chain conformational renormalization group method is applied to the calculation of the distribution functions for intersegment distance vectors, the mean square intersegment distances, the mean square radius of gyration, the osmotic second virial coefficient, and the interpenetration function for f -branched star polymers. The calculations provide the full crossover dependence of all quantities on the strength of the excluded volume interaction and the chain length. The results provide a picture of excluded volume effects on the conformations of star polymers which is rather different from that assumed in recent scaling models. Some of the important information concerning the structure of the star polymers emerges from the prefactors since many power law exponents are independent of the number of branches, thereby emphasizing the importance of evaluating these prefactors.

I. Introduction

Star polymers have been attracting a considerable

amount of experimental and theoretical interest. Experimental work in dilute solutions has been performed by light scattering¹⁻³ and by the measurement of hydrodynamic and rheological properties.⁴⁻⁶ In addition, a number of experiments have focused on star polymers in concen-

[†] On leave of absence from the Department of Physics, International Christian University, Tokyo.

trated solutions and melts, but it is in the dilute solution limit where polymer characterization is generally made.

The complexity of star polymers has led much of the theoretical work⁷⁻¹¹ to be concerned with the conformational statistics of star polymers in Θ solvents, despite the likelihood that a many-branched star polymer may not have a simple Θ point because of the very high monomer density in the neighborhood of the center of the star. Naturally, the theoretical focus on ideal solutions of star polymers has been accompanied by experimental efforts in Θ solutions. Here we emphasize how the study of star polymers in good solutions for varying numbers of branches can help to provide the wealth of data necessary to firmly test theories of polymer excluded volume.

Recently, Daoud and Cotton¹² have proposed a model for the conformation of star polymers in good solvents on the basis of blob concepts^{13,14} and a geometric-type model for the average chain structure. Their model *assumes* the blob size, and consequently the monomer concentration, to be a monotonically decreasing function of the distance from the center (i.e., internal branch point) of the star. This assumption combined with the blob-type arguments indicates the presence of three different regimes as a function of the radial distance from the star's center. These regions are (1) a close-packed core of constant monomer density, (2) a high monomer concentration intermediate zone where the excluded volume interaction is screened so the chain segments are Gaussian, and (3) a lower monomer concentration exterior where excluded volume effects are present within the blobs. Some of their predicted results are found to be in good agreement with experiment.¹ However, they have assumed a rather ad hoc geometrical model of the star polymer involving assumptions of the size of the blobs as a function of the distance from the star center which remain to be tested on the basis of a rigorous theory. In addition, were this blob model to be precisely correct, it would still suffer from the deficiencies of all blob-model calculations. These treatments are based upon scaling theories that describe only the asymptotic limit of long enough chains (here star arms) and strong enough excluded volume. The criteria for the occurrence of this idealized limit cannot be given by the scaling theory nor can corrections to the limiting behavior. Moreover, the scaling theories focus only on molecular weight and concentration power law exponents, ignoring the important prefactors and distribution functions. The blob models cannot properly describe the crossover region between the Gaussian chain limit and the idealized excluded volume limit, and a more rigorous and theoretically well founded theory is required to alleviate these deficiencies of the scaling method.

Here we provide a test of the Daoud-Cotton model of star polymers as well as detailed calculations of a wealth of properties of star polymers with excluded volume using the renormalization group method. The chain conformational renormalization group approach has been shown to be powerful enough to enable the calculation of interesting polymer distributions such as that for the end-to-end vector,¹⁵ internal vectors,^{16,17} and the coherent scattering function.¹⁸ Furthermore, the theory properly provides the crossover behavior between the Gaussian and self-avoiding chain limits.¹⁹ The calculations are designed to provide further insight into the effects of branching in polymers, and other geometrical branching structures like comb polymers, etc., can readily be handled by the same methods. The current theory is limited to situations where the local monomer density is not so high that considerations of packing become relevant. This is because the traditional continuum excluded volume theories describe excluded volume by point interactions, while at high volume frac-

tions (>20-30%) the hard-core packing volume of the monomers becomes a relevant parameter that cannot be ignored. Experimental data suggest that this traditional theory is applicable for star polymers with up to 6 or 7 branches, so corrections for packing volume are probably necessary for a larger number of branches.

We utilize a Gell-Mann-Low type renormalization procedure²⁰ in chain conformation space with the cutoff a retained¹⁸ as opposed to the dimensional regularization technique.¹⁵ The general theoretical background is summarized in section II in a physical fashion that displays the conceptual framework of the theory. The distribution function for intersegment distances is evaluated for pairs of segments lying on the same or different branches in section III. The full crossover results are given as a function of the branch lengths and the strength of the excluded volume interaction. This provides the effective exponents ν for the mean square chain size and γ for the number of chain conformations as a function of the number of branches f and the crossover variable ζ . The mean square intersegmental distances and the mean square radius of gyration are then readily determined in section IV from the distributions. The results vividly display the combined effects of chain branching and excluded volume, and a picture rather different from the Daoud-Cotton model emerges out of this detailed information concerning the structure of star polymers. This picture is discussed in detail in section VI after calculations of the osmotic second virial coefficient and the interpenetrating function are presented in section V. The calculational methods have been extensively explained in previous papers,¹⁵⁻¹⁹ so they are not provided in detail. We present all the diagrams and their computed values in the appendices for those who are interested in some of the lengthy theoretical details. Otherwise, we quote the results of the lengthy calculations and display some of them graphically.

II. Theoretical Background

Here we summarize the basic features of the chain conformational space renormalization group method necessary to define the model and to provide a physical understanding of the method. Details of the theoretical procedure are given in a series of previous papers¹⁵⁻¹⁹ for interested readers.

The model of a star polymer employed here is that of a continuous chain with f branches joined at the center, which is taken to be at the origin of the coordinate system. The polymer has excluded volume and would reduce to a Gaussian star polymer for vanishing excluded volume. Let $\mathbf{r}(\tau_i)$ designate the position of the chain segment at a contour distance τ_i along the i th branch. τ_i increases from the star center at the position $\mathbf{r}(\tau_i=0) = 0$. For convenience, we take all branches to be of equal length to simplify the algebraic expressions, but the unequal arm length case is readily extracted from the given calculations in the appendices.

A convenient configurational variable is taken as

$$\mathbf{c}(\tau_i) = (d/l)^{1/2} \mathbf{r}(\tau_i) \quad (2.1)$$

with d the dimensionality of space and l the Kuhn effective step length. The dimensionless Hamiltonian is written in terms of $\mathbf{c}(\tau_i)$ as

$$H_a = \frac{1}{2} \sum_{i=1}^f \int_0^{N_0} d\tau_i [d\mathbf{c}(\tau_i)/d\tau_i]^2 + \frac{1}{2} v_0 \sum_{i=1}^f \int_0^{N_0} \int_0^{N_0} d\tau_i d\tau'_i \delta[\mathbf{c}(\tau_i) - \mathbf{c}(\tau'_i)] + \frac{1}{2} v_0 \sum_{i \neq j=1}^f \int_0^{N_0} \int_0^{N_0} d\tau_i d\tau_j \delta[\mathbf{c}(\tau_i) - \mathbf{c}(\tau_j)] \quad (2.2)$$

where N_0 is the length of each branch of the continuous star polymer model, v_0 is the microscopic bare excluded volume describing binary interactions between units, and a is a cutoff contour length to eliminate contributions from self-excluded volume interactions. Equation 2.2 contains three terms: the first term is the entropic contribution providing chain connectivity, while the second and third terms, respectively, involve intra- and interbranch excluded volume interactions.

Consider a microscopic function of the chain conformation $Q[\mathbf{c}(\tau_i)]$ for which a long-wavelength macroscopic average Q exists. A bare, unrenormalized expectation value Q_B is obtained from the model (2.2) in the usual fashion $Q_B(v_0, N_0, f, a) = \int D[\mathbf{c}(\tau_i)] Q[\mathbf{c}(\tau_i)] \exp\{-H_a[\mathbf{c}(\tau_i)]\} \quad (2.3)$

where $D[\mathbf{c}(\tau_i)]$ is the integration measure for the continuous Gaussian chain.²⁰ Since Q_B is not necessarily properly normalized, the observable Q may differ from Q_B by a normalization constant

$$Q = Z_Q Q_B(v_0, N_0, f, a) \quad (2.4)$$

where Z_Q also serves the renormalization role of eliminating from Q_B some sensitive microscopic dependences therein which cannot be present in the long-wavelength macroscopic limit. This arises because the calculated Q_B of (2.3) is found to be a singular function of the cutoff a in the limit $a \rightarrow 0$, and it is a central reason for the need for normalization. Examples of (2.3) and (2.4) are presented in section III.

The microscopic model displays the correct long-wavelength properties of the polymers, but the continuous chain model is clearly incorrect over short distances. Hence, the actual branch length N , proportional to the molecular weight, need not be identical with the model length N_0 . Since, say, doubling N_0 should double N , they must be proportional to each other

$$N = Z_2 N_0 \quad (2.5)$$

Note that (2.5) is just a particular example of (2.4). Z_2 therefore depends on microscopic details like a .

The bare excluded volume v_0 in (2.2) describes a binary encounter between a pair of segments, whereas on a macroscopic coarse-grained length scale L the cooperative effects of excluded volume are summarized through the macroscopic excluded volume v , which must be independent of N_0 (or N). It is convenient to introduce the dimensionless variables

$$u_0 = v_0 L^{\epsilon/2}, \quad u = v L^{\epsilon/2} \quad (2.6)$$

where $\epsilon = 4 - d$.

The relation between these macroscopic and microscopic interaction parameters may be expressed as

$$u = u(u_0, a/L) \quad (2.7)$$

a/L is the only other dimensionless variable not involving N_0 or N that may be constructed from the model.

Q_B from (2.3) is obviously independent of L , since L appears nowhere in $Q[\mathbf{c}(\tau_i)]$ or $H_a[\mathbf{c}(\tau_i)]$. Hence, we have the trivial statement

$$\left[L \frac{\partial}{\partial L} Q_B(v_0, N_0, f, a) \right]_{v_0, N_0, f, a} = 0 \quad (2.8)$$

However, inserting the macroscopic-microscopic relations from (2.5) and (2.7) into (2.3) and noting that the dimensionless Z_2 and Z_Q (2.4) depend on u and a/L enable (2.8) to be transformed into the highly nontrivial renormalization group (RG) equations²¹

$$\left[L \frac{\partial}{\partial L} + \beta(u) \frac{\partial}{\partial u} - L \frac{\partial \ln Z_Q}{\partial L} + L \frac{\partial \ln Z_2}{\partial L} N \frac{\partial}{\partial N} \right]_{v_0, N_0, f, a} Q(u, N, f, L) = 0 \quad (2.9)$$

with the Gell-Mann-Low function

$$\beta(u) = L \frac{\partial u}{\partial L} \Big|_{v_0, N_0, f, a} \quad (2.10)$$

The general solution of (2.8) is¹⁹

$$Q(u, N, f, L) = \exp \left[\int_{u_1}^u \frac{\gamma_1(x)}{\beta(x)} dx \right] \times F \left(N \exp \left[- \int_{u_1}^u \frac{\gamma_2(x)}{\beta(x)} dx \right], L \exp \left[- \int_{u_1}^u \frac{dx}{\beta(x)} \right] \right) \quad (2.11)$$

where

$$\gamma_1(u) = L \frac{\partial \ln Z_Q}{\partial L} \Big|_{v_0, N_0, f, a} \quad (2.12)$$

$$\gamma_2(u) = L \frac{\partial \ln Z_2}{\partial L} \Big|_{v_0, N_0, f, a} \quad (2.13)$$

F is an arbitrary well-behaved function to be determined, and u_1 is an arbitrary macroscopic parameter that may be chosen conveniently along with F . The function F is ultimately specified by comparison with the renormalized calculated Q_B from (2.3). The combination of (2.11) with simple dimensional analysis of Q enables the scaling form of Q to be derived under the conditions that either $N \rightarrow \infty$ for $u \neq 0$ or $u \rightarrow u^*$ such that $\beta(u^*) = 0$. However, the general case of (2.11) is valid even when this scaling limit is not met.

One of the previous papers¹⁸ pursues the analysis with a small but nonzero a such that $a/L \ll 1$. In this case the quantities Q_B are found to display a singular dependence on a/L . Hence, Z_Q , Z_2 , and $u(u_0, a/L)$ are chosen to absorb all these singular terms in order that $Q(u, N, f, L)$ is independent of these microscopic detailed singularities. It is readily found that $u(u_0, a/L)$ must be the same for the linear and star polymers, so we quote the results¹⁸

$$u = u_0 + \frac{u_0^2}{\pi^2} \ln(2\pi a/L) + \dots \quad (2.7a)$$

(This is because the star and linear polymers belong to the same universality class.) Substituting (2.6) and (2.7a) into the definition (2.10) of $u_0(u)$ yields

$$\beta(u) = \frac{\epsilon}{2} u - \frac{u^2}{\pi^2} + \mathcal{O}(u^3, u^2 \epsilon) \quad (2.14)$$

Hence, the scaling limit ensues for arbitrary macroscopic N whenever $u = u^*$, with

$$u^* = \frac{\epsilon}{2} \pi^2 + \mathcal{O}(\epsilon^2) \quad (2.15)$$

It should be noted that the calculations proceed by the traditional excluded volume perturbation expansion²⁰ in powers of v_0 with subsequent expansion in $\epsilon = 4 - d$. The latter is introduced because the perturbation expansion is well-known to be a series in the dimensionless variable $v_0 N_0^{\epsilon/2}$, which is of little use for long polymers $N_0 \rightarrow \infty$. However, the subsequent ϵ expansion

$$v_0 N_0^{\epsilon/2} = v_0 \left\{ 1 + \frac{\epsilon}{2} \ln N_0 + \frac{\epsilon^2}{8} (\ln N_0)^2 + \dots \right\} \quad (2.16)$$

gives the controllable expansion parameter $\epsilon \ln N_0$ for ϵ small and N_0 large. The RG equation (2.9) provides the means for extending the calculation for $\epsilon \ll 1$ to the physically interesting domain of $\epsilon = 1$. For instance, the radius of gyration R_G is predicted from (2.11) to have the scaling form $R_G = bN^\nu$ for $u = u^*$ or $N \rightarrow \infty$ for $u \neq 0$. If the ϵ expansion yields $R_G = bN^{1/2}[1 + m\epsilon \ln N + \mathcal{O}(\epsilon^2)]$, then to order ϵ this implies $\nu = 1/2 + m\epsilon$, etc. Note that the actual expansion parameter turns out to be $\epsilon/8$. The details of this type of analysis have been given previously,¹⁵⁻¹⁹ so we do not give them again in the present context.

III. Distribution Functions for Intersegment Distance Vectors

A. Case Where Both Segments Lie on the Same Branch. Recall that the star center is taken as the origin of the coordinate system. Consider two segments located at contour distances N_0x and N_0y along the same branch and let their spatial positions be \mathbf{r}_1 and \mathbf{r}_2 , respectively. We seek the two fixed-segment partition functions $G(\mathbf{r}_1, \mathbf{r}_2, x, y; u, N, f, L)$ with $\mathbf{r} = \mathbf{r}_2 - \mathbf{r}_1$. When normalized, G is converted to the intrabranched internal vector distribution function.

The bare distribution function is evaluated as a specific example of (2.3) as

$$G_B(\mathbf{r}, x, y; u_0, N_0, f, a) = \int d\mathbf{r}_1 \int d[\mathbf{c}(\tau_i)] \delta[\mathbf{c}(N_0x) - (d/l)^{1/2}\mathbf{r}_1] \delta[\mathbf{c}(N_0y) - (d/l)^{1/2}(\mathbf{r}_1 + \mathbf{r})] \exp[-H_a[\mathbf{c}(\tau_i)]] \quad (3.1)$$

with H_a given in (2.2). The perturbation expansion of (3.1) to order v_0 is written as

$$G_B(\mathbf{r}, x, y; u_0, N_0, f, a) = G_0(\mathbf{c}, N_0(y-x)) - v_0 G_1(\mathbf{c}, N_0x, N_0y) + \mathcal{O}(v_0^2) \quad (3.2)$$

where the zeroth-order Gaussian distribution in $d = 4 - \epsilon$ dimensions is

$$G_0(\mathbf{c}, N_0(y-x)) = [2\pi N_0(y-x)]^{-2+\epsilon/2} \exp[-\mathbf{c}^2/2N_0(y-x)] \quad (3.3)$$

The individual contributions to G_1 are given in Appendix A, where they are represented diagrammatically. The terms in (A.1)–(A.6) are identical with those for a linear polymer of bare length N_0 , while those in (A.7)–(A.10) would be for a linear polymer of bare length $2N_0$. The terms (A.7)–(A.10), however, enter with weights of $f-1$. Only (A.11) is a fundamentally new diagram for the branched polymer. Appendix A presents the values of each diagram after an expansion in ϵ through order ϵ^0 , where we obtain

$$G_1(\mathbf{c}, N_0x, N_0y) = G_0(\mathbf{c}, N_0(y-x)) \frac{1}{(2\pi)^2} \left[\frac{fN_0}{a} - (\alpha_0 - 1) \ln \frac{N_0}{a} + \frac{(f-1)(f-2)}{2} \ln \frac{N_0}{a} + 1 - 3\gamma - \ln x - \ln(1-y) + 3 \ln(y-x) + \frac{2}{\alpha_0} - \alpha_0 \{1 + \ln(y-x) - (\gamma + \ln \alpha_0)\} - 3 \ln \alpha_0 + \frac{1}{\alpha_0(y-x)} \left\{ (1+x-y) \exp\left(-\alpha_0 \frac{y-x}{1+x-y}\right) - y \exp\left(-\alpha_0 \frac{y-x}{x}\right) - (1-x) \exp\left(-\alpha_0 \frac{y-x}{1-y}\right) \right\} + E_1\left(\alpha_0 \frac{y-x}{x}\right) + E_1\left(\alpha_0 \frac{y-x}{1-y}\right) - E_1\left(\alpha_0 \frac{y-x}{1+x-y}\right) - \right.$$

$$F\left(\alpha_0; \frac{x}{y-x}\right) - F\left(\alpha_0; \frac{1-y}{y-x}\right) + (f-1) \left\{ \ln x - \ln(1+x) + \frac{1}{\alpha_0(y-x)} \left[(2+x-y) \exp\left(-\alpha_0 \frac{y-x}{2+x-y}\right) - (1+x-y) \exp\left(-\alpha_0 \frac{y-x}{1+x-y}\right) - (1+y) \times \exp\left(-\alpha_0 \frac{y-x}{1+x}\right) + y \exp\left(-\alpha_0 \frac{y-x}{x}\right) \right] + E_1\left(\alpha_0 \frac{y-x}{1+x-y}\right) - E_1\left(\alpha_0 \frac{y-x}{2+x-y}\right) - E_1\left(\alpha_0 \frac{y-x}{x}\right) + E_1\left(\alpha_0 \frac{y-x}{1+x}\right) + F\left(\alpha_0; \frac{x}{y-x}\right) - F\left(\alpha_0; \frac{1+x}{y-x}\right) \right\} + \frac{(f-1)(f-2)}{2} (1 - \ln 2) \quad (3.4)$$

where

$$\alpha_0 = \mathbf{c}^2/2N_0(y-x) \quad (3.5)$$

$$E_1(x) = \int_x^\infty e^{-t} dt/t = \int_0^x (1-e^{-t}) dt/t - \ln x - \gamma \quad (\text{exponential integral}^{22}) \quad (3.6)$$

$$F(\alpha_0; \lambda) = \int_0^1 dt \frac{t+2\lambda}{\{t(1-t)+\lambda\}^2} \exp\left\{-\frac{\alpha_0 t^2}{t(1-t)+\lambda}\right\} \quad (3.7)$$

and γ is Euler's constant.

Equation 3.4 has terms that become singular in the limit $a/L \rightarrow 0$, thereby displaying a sensitivity to microscopic details that should not be present in the long-wavelength observable G . Contributions in N_0/a enter in the form of a portion of the chain free energy, so these terms can be absorbed into the definition of the zero of energy by $v_0 f N_0 / 4\pi^2 a$. The logarithmic terms in a/L are more significant and are absorbed into the definitions of Z_G and Z_2 of

$$Z_G = 1 - \frac{u}{(2\pi)^2} \left\{ \frac{(f-1)(f-2)}{2} - 1 \right\} \ln \frac{2\pi a}{L} + \dots \quad (3.8)$$

$$Z_2 = 1 - \frac{u}{(2\pi)^2} \ln \frac{2\pi a}{L} + \dots \quad (3.9)$$

so that the renormalized G [cf. (2.4)] of

$$G(\mathbf{r}, x, y; u, N, f, L) = Z_G G_B(\mathbf{r}, x, y; u_0(u) L^{-\epsilon/2}, Z_2^{-1} N, f, a) \quad (3.10)$$

is free of singular terms as $a/L \rightarrow 0$.

Note that Z_2 is identical with that for linear polymers,¹⁸ and hence $\gamma_2(u)$ of (2.13) is also the same

$$\gamma_2(u) = \frac{u}{(2\pi)^2} + \mathcal{O}(u^2) \quad (3.11)$$

Therefore, eq 2.11 indicates that G must be written in terms of the same scaling variables as for linear polymers¹⁹

$$\zeta = (2\pi N/L)^{\epsilon/2} \bar{u}(1-\bar{u})^{-1+\epsilon/8} \quad (3.12)$$

$$X = \mathbf{c}^2(1-\bar{u})^{-1/4}/2N = (\mathbf{c}^2/2N)[1 + \zeta(1+\zeta)^{\epsilon/8}]^{1/2} (2\pi N/L)^{-(\epsilon/8)[\zeta/(1+\zeta)]} \quad (3.13)$$

where

$$\bar{u} = u/u^* \quad (3.14)$$

and $\bar{u} = 0$ implies $\zeta = 0$ gives the Gaussian chain limit, whereas $\bar{u} = 1$ implies $\zeta = \infty$ gives the asymptotic self-avoiding limit of fully developed excluded volume. Equation 3.13 involves the effective ζ -dependent exponent

$$2\nu(\zeta) = 1 + \frac{\epsilon}{8} \frac{\zeta}{1 + \zeta} \quad (3.15)$$

Since G produces a distribution function when normalized, it must be a nonnegative quantity. The simple traditional perturbation expansion (3.2) does not generally preserve this essential property, but this difficulty is simply remedied by utilizing instead a perturbation expansion of $\ln G$ in powers of ν_0 and ϵ . To lowest order this merely implies the exponentiation of the first-order terms to give

$$\begin{aligned} G(\alpha, x, y; u, N, L) = & (2\pi N/L)^{-(\epsilon/8)[\zeta/(1+\zeta)] + (f-1)(f-2)/2} \{2\pi N(y-x)\}^{-2+\epsilon/2} \times \\ & \exp\left[-\alpha - \frac{\epsilon}{8} \frac{\zeta}{1 + \zeta} \left[2 - 3\gamma - \ln x - \ln(1-y) + \right. \right. \\ & \left. \left. 3 \ln(y-x) + \frac{2}{\alpha} - \alpha\{1 + \ln(y-x) - (\gamma + \ln \alpha)\} - \right. \right. \\ & \left. \left. 3 \ln \alpha + \frac{1}{\alpha(y-x)}\right\} (1+x-y) \times \right. \\ & \left. \exp\left(-\alpha \frac{y-x}{1+x-y}\right) - y \exp\left(-\alpha \frac{y-x}{x}\right) - \right. \\ & \left. (1-x) \exp\left(-\alpha \frac{y-x}{1-y}\right)\right\} + \\ & E_1\left(\alpha \frac{y-x}{x}\right) + E_1\left(\alpha \frac{y-x}{1-y}\right) - E_1\left(\alpha \frac{y-x}{1+x-y}\right) - \\ & F\left(\alpha; \frac{1-y}{y-x}\right) - F\left(\alpha; \frac{x}{y-x}\right) + (f-1) \left\{ \ln 2 + \ln x - \right. \\ & \left. \ln(1+x) + \frac{1}{\alpha(y-x)} \left[(2+x-y) \times \right. \right. \\ & \left. \left. \exp\left(-\alpha \frac{y-x}{2+x-y}\right) - (1+x-y) \times \right. \right. \\ & \left. \left. \exp\left(-\alpha \frac{y-x}{1+x-y}\right) - (1+y) \exp\left(-\alpha \frac{y-x}{1+x}\right) + \right. \right. \\ & \left. \left. y \exp\left(-\alpha \frac{y-x}{x}\right) \right] \right\} + \\ & E_1\left(\alpha \frac{y-x}{1+x-y}\right) - E_1\left(\alpha \frac{y-x}{2+x-y}\right) - E_1\left(\alpha \frac{y-x}{x}\right) + \\ & E_1\left(\alpha \frac{y-x}{1+x}\right) - F\left(\alpha; \frac{x}{y-x}\right) - F\left(\alpha; \frac{1+x}{y-x}\right) \} \quad (3.16) \end{aligned}$$

where we have the definition

$$\alpha = X[1 + \zeta(1 + \zeta)^{\epsilon/8}]^{-1/4} / (y-x) = \{c^2/2N(y-x)\} (2\pi N/L)^{-(\epsilon/8)[\zeta/(1+\zeta)]} \quad (3.17)$$

When $f = 1$ and when (3.16) is taken in the asymptotic scaling limit $\zeta \rightarrow \infty$, then (3.16) reduces to the previous result.¹⁷ Equation 3.16, hence, provides the appropriate crossover generalization for a linear polymer by taking $f = 1$ and $\zeta \neq \infty$, but this case could readily be obtained by

introducing the techniques of ref 19 into ref 17. Note that the correspondence between the $f = 1$, $\zeta = \infty$ limit of (3.16) and the linear-chain case¹⁷ is obtained with the aid of the relations

$$\begin{aligned} F(\alpha; \lambda) = & \frac{1}{\alpha} [1 - \exp(-\alpha/\lambda)] - \\ & \frac{1}{\alpha} \int_0^1 \left\{ \exp\left[-\frac{\alpha t^2}{t(1-t) + \lambda}\right] - 1 \right\} dt/t^2 \quad (3.18) \end{aligned}$$

$$E_1(x) = -E_1(-x) \quad (3.19)$$

B. Case Where Both Segments Lie on Different Branches. Now let $\mathbf{r} = \mathbf{r}_2 - \mathbf{r}_1$ again and take the segments at \mathbf{r}_1, N_0x and \mathbf{r}_2, N_0y to lie on different branches. The diagrams for G_B' in this case are given in Appendix B. Those in (B.1)–(B.6) could be extracted from a linear-chain calculation with a chain of bare length $2N_0$. The contributions (B.7)–(B.12) are particular to star polymers. The perturbation expansion is of the same form as (3.2) with G_B' and G_1' , respectively, replacing G_B and G_1 . Collecting terms from Appendix B yields

$$\begin{aligned} G_1'(\mathbf{c}, N_0x, N_0y) = & G_0(\mathbf{c}, N_0(x+y)) \frac{1}{(2\pi)^2} \left[\frac{fN_0}{a} - (\alpha_0 - 1) \ln \frac{N_0}{a} + \right. \\ & \left. \frac{(f-1)(f-2)}{2} \ln \frac{N_0}{a} + 1 - 3\gamma - \ln(1-x) - \right. \\ & \left. \ln(1-y) + 3 \ln(x+y) + \frac{2}{\alpha_0} - 3 \ln \alpha_0 - \right. \\ & \left. \alpha_0\{1 + \ln(x+y) - (\gamma + \ln \alpha_0)\} + \right. \\ & E_1\left(\alpha_0 \frac{x+y}{1-x}\right) + E_1\left(\alpha_0 \frac{x+y}{1-y}\right) - E_1\left(\alpha_0 \frac{x+y}{2-x-y}\right) - \\ & F\left(\alpha_0; \frac{1-y}{x+y}\right) - F\left(\alpha_0; \frac{1-x}{x+y}\right) + \frac{1}{\alpha_0(x+y)} \left\{ (2-x-y) \right. \\ & \left. \exp\left(-\alpha_0 \frac{x+y}{2-x-y}\right) - (1+y) \exp\left(-\alpha_0 \frac{x+y}{1-x}\right) - \right. \\ & \left. (1+x) \exp\left(-\alpha_0 \frac{x+y}{1-y}\right) \right\} + \\ & (f-2) \left\{ 3 - 2\gamma + \frac{2}{\alpha_0} - 2 \ln \alpha_0 + 2 \ln(x+y) + \right. \\ & \left. \frac{1}{\alpha_0 x^2} \left[\{2(x+y) - x^2\} \exp\left(-\frac{\alpha_0 x^2}{2(x+y) - x^2}\right) - \right. \right. \\ & \left. \left. (x+y-x^2) \exp\left(-\frac{\alpha_0 x^2}{x+y-x^2}\right) - \right. \right. \\ & \left. \left. \{(x+y)(1+x) + xy\} \exp\left(-\frac{\alpha_0 x^2}{x+y+xy}\right) \right] + \right. \\ & \left. \frac{2y}{\alpha_0 x} \exp\left(-\frac{\alpha_0 x}{y}\right) - E_1\left(\frac{\alpha_0 x^2}{2(x+y) - x^2}\right) + \right. \\ & E_1\left(\frac{\alpha_0 x^2}{x+y-x^2}\right) + E_1\left(\frac{\alpha_0 x^2}{x+y+xy}\right) - 2E_1\left(\frac{\alpha_0 x}{y}\right) + \\ & \left. \frac{1}{\alpha_0 y^2} \left[\{2(x+y) - y^2\} \exp\left(-\frac{\alpha_0 y^2}{2(x+y) - y^2}\right) - \right. \right. \end{aligned}$$

$$\begin{aligned}
& (x+y-y^2) \exp\left(-\frac{\alpha_0 y^2}{x+y-y^2}\right) - \{(x+y)(1+y) + \\
& xy\} \exp\left(-\frac{\alpha_0 y^2}{x+y+xy}\right) \Bigg] + \frac{2x}{\alpha_0 y} \exp\left(-\frac{\alpha_0 y}{x}\right) - \\
& E_1\left(\frac{\alpha_0 y^2}{2(x+y)-y^2}\right) + \\
& E_1\left(\frac{\alpha_0 y^2}{x+y-y^2}\right) + E_1\left(\frac{\alpha_0 y^2}{x+y+xy}\right) - 2E_1\left(\frac{\alpha_0 y}{x}\right) - \\
& F'(\alpha_0; x) - F'(\alpha_0; y) \Bigg\} + \frac{(f-2)(f-3)}{2} (1 - \ln 2) \Bigg] \quad (3.4')
\end{aligned}$$

where

$$\alpha_0 = c^2/2N_0(x+y) \quad (3.5')$$

$$\begin{aligned}
F'(\alpha_0; \lambda) = (x+y)^2 \int_0^\lambda \frac{(t+2) dt}{\{(x+y)(1+t) - t^2\}^2} \times \\
\exp\left\{-\frac{\alpha_0 t^2}{(x+y)(1+t) - t^2}\right\} \quad (3.7')
\end{aligned}$$

We now follow the same techniques as in section IIIA to obtain the unnormalized interbranch intersegment vector distribution to first order in ϵ as

$$\begin{aligned}
G'(\alpha, x, y; u, N, L) = & \left(\frac{2\pi N}{L}\right)^{-(\epsilon/8)[f/(1+f)]} [2\pi N(x+y)]^{-2+\epsilon/2} \times \\
& \exp\left[-\alpha - \frac{\epsilon}{8} \frac{\zeta}{1+\zeta} \left[2 - 3\gamma + \ln 2 - \right. \right. \\
& \ln(1-x) - \ln(1-y) + 3 \ln(x+y) + \frac{2}{\alpha} - 3 \ln \alpha - \\
& \alpha\{1 - \gamma + \ln(x+y)\} + \alpha \ln \alpha - F\left(\alpha; \frac{1-x}{x+y}\right) - \\
& F\left(\alpha; \frac{1-y}{x+y}\right) + E_1\left(\alpha \frac{x+y}{1-x}\right) - \\
& E_1\left(\alpha \frac{x+y}{2-x-y}\right) + \\
& \frac{1}{\alpha(x+y)} \left\{ (2-x-y) \exp\left(-\alpha \frac{x+y}{2-x-y}\right) - \right. \\
& (1+y) \exp\left(-\alpha \frac{x+y}{1-x}\right) - (1+x) \exp\left(-\alpha \frac{x+y}{1-y}\right) \Bigg\} + \\
& (f-2)\{2 - 2\gamma + 2 \ln 2 + 2 \ln(x+y) + \frac{2}{\alpha} - 2 \ln \alpha + \\
& \frac{1}{\alpha x^2} \left[\{2(x+y) - x^2\} \exp\left(-\frac{\alpha x^2}{2(x+y) - x^2}\right) - \right. \\
& (x+y-x^2) \exp\left(-\frac{\alpha x^2}{x+y-x^2}\right) - \\
& \left. \left. \{(x+y)(1+x) + xy\} \exp\left(-\frac{\alpha x^2}{x+y+xy}\right) \right] + \right. \\
& \left. \frac{2y}{\alpha x} \exp\left(-\frac{\alpha x}{y}\right) - E_1\left(\frac{\alpha x^2}{2(x+y) - x^2}\right) + \right.
\end{aligned}$$

$$\begin{aligned}
& E_1\left(\frac{\alpha x^2}{x+y-x^2}\right) + E_1\left(\frac{\alpha x^2}{x+y+xy}\right) - 2E_1\left(\frac{\alpha x}{y}\right) + \\
& \frac{1}{\alpha y^2} \left[\{2(x+y) - y^2\} \exp\left(-\frac{\alpha y^2}{2(x+y) - y^2}\right) - \right. \\
& (x+y-y^2) \exp\left(-\frac{\alpha y^2}{x+y-y^2}\right) - \\
& \left. \{(x+y)(1+y) + xy\} \exp\left(-\frac{\alpha y^2}{x+y+xy}\right) \right] + \\
& \frac{2x}{\alpha y} \exp\left(-\frac{\alpha y}{x}\right) - E_1\left(\frac{\alpha y^2}{2(x+y) - y^2}\right) + \\
& E_1\left(\frac{\alpha y^2}{x+y-y^2}\right) + E_1\left(\frac{\alpha y^2}{x+y+xy}\right) - \\
& 2E_1\left(\alpha \frac{y}{x}\right) - F'(\alpha; x) - F'(\alpha; y) \Bigg] \quad (3.16')
\end{aligned}$$

where

$$\begin{aligned}
\alpha = X[1 + \zeta(1 + \zeta)^{\epsilon/8}]^{-1/4} / (x+y) = \\
\{c^2/2N(x+y)\} (2\pi N/L)^{-(\epsilon/8)[f/(1+f)]} \quad (3.17')
\end{aligned}$$

It is readily seen that (3.16') reduces to the linear polymer case of a chain of length $2N$ when $f = 2$.

C. Total Number of Conformations and Normalization. The distribution functions G and G' are normalized by dividing by the quantity

$$\int d\mathbf{r} G(\mathbf{r}, x, y; u, N, f, L) = CN^{\gamma_f-1} \quad (3.20)$$

giving the total number of star polymer conformations between the segments x and y relative to that for a Gaussian star polymer. Since the zeroth-order G_0 is normalized

$$\int d\mathbf{c} G_0(\mathbf{c}, N_0(y \pm x)) = 1 \quad (3.21)$$

using (3.17) or (3.17'), we obtain

$$\begin{aligned}
\int d\mathbf{c} G(\mathbf{c}, x, y; u, N, f, L) = \int_0^\infty G(\alpha, x, y; u, N, L) \alpha^{1-\epsilon/2} d\alpha \\
[2N(y-x)]^{2-\epsilon/2} \left(\frac{2\pi N}{L}\right)^{(\epsilon/4)[f/(1+f)]} = \\
\int_0^\infty G'(\alpha, x, y; u, N, L) \alpha^{1-\epsilon/2} d\alpha [2N(x+y)]^{2-\epsilon/2} \left(\frac{2\pi N}{L}\right)^{(\epsilon/4)[f/(1+f)]} \\
\propto N^{(\epsilon/8)[f/(1+f)]} [1 - (f-1)(f-2)/2] \quad (3.22)
\end{aligned}$$

giving the effective exponent in the crossover regime

$$\gamma_f = 1 + \frac{\epsilon}{8} \frac{\zeta}{1+\zeta} \left\{ 1 - \frac{(f-1)(f-2)}{2} \right\} \quad (3.23)$$

$\gamma_{f=1}$ and $\gamma_{f=2}$ coincide with the linear polymer result.¹⁵ It is interesting that the coefficient of ϵ vanishes for $f = 3$ and becomes negative for $f \geq 4$. This indicates a crowding effect due to the presence of many branches that leads to a diminution of the number of chain conformations.

IV. Mean Square Intersegment Distance and Radius of Gyration

The calculation of the mean square intersegment distance follows straightforwardly from section III by integration. Using (3.16), (3.17), and (2.1) yields for two segments on the same branch

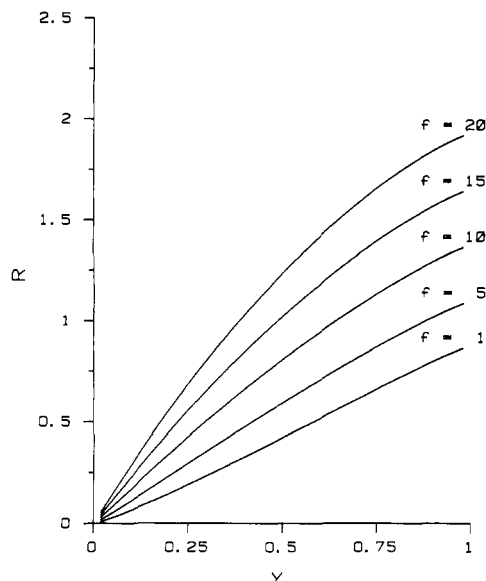


Figure 1. $R = \langle r^2 \rangle_{0,y} / Nl(2\pi N/L)^{1/8}$ vs. y in the self-avoiding limit for different values of f , the number of branches. $\langle r^2 \rangle_{0,y}$ is the mean square distance of a segment located at the contour distance Ny along a branch from the center of a star polymer.

$$\begin{aligned} \langle r^2 \rangle_{x,y} &= \frac{l}{d} 2N(y-x)(2\pi N/L)^{(\epsilon/8)[\zeta/(1+\zeta)]} \times \\ &\quad \int_0^\infty G(\alpha, x, y; u, N, L) \alpha^{2-\epsilon/2} d\alpha / \\ &\quad \int_0^\infty G(\alpha, x, y; u, N, L) \alpha^{1-\epsilon/2} d\alpha = Nl(2\pi N/L)^{(\epsilon/8)[\zeta/(1+\zeta)]} (y-x) \\ &\quad x^{1+(\epsilon/8)[\zeta/(1+\zeta)]} \left[1 - \frac{\epsilon}{8} \frac{\zeta}{1+\zeta} \left\{ 1 - \frac{x}{y-x} \ln y - \frac{1-y}{y-x} \ln \right. \right. \\ &\quad \left. \left. (1-x) + \frac{1-y}{y-x} \ln(1-y) + \frac{x}{y-x} \ln x + \frac{1+x-y}{2} + \right. \right. \\ &\quad \left. \left. (f-1) \left[\frac{y-x}{4} + \frac{x}{y-x} \ln y - \frac{x}{y-x} \ln x - \right. \right. \right. \\ &\quad \left. \left. \left. \frac{1+x}{y-x} \ln(1+y) + \frac{1+x}{y-x} \ln(1+x) \right] \right\} \right] \quad (4.1) \end{aligned}$$

When the segments are on different branches, combining (3.16'), (3.17'), and (2.1) produces

$$\begin{aligned} \langle r^2 \rangle_{x,y'} &= \frac{l}{d} 2N(x+y)(2\pi N/L)^{(\epsilon/8)[\zeta/(1+\zeta)]} \times \\ &\quad \int_0^\infty G'(\alpha, x, y; u, N, L) \alpha^{2-\epsilon/2} d\alpha / \\ &\quad \int_0^\infty G'(\alpha, x, y; u, N, L) \alpha^{1-\epsilon/2} d\alpha = \\ &\quad Nl(2\pi N/L)^{(\epsilon/8)[\zeta/(1+\zeta)]} (x+y)^{1+(\epsilon/8)[\zeta/(1+\zeta)]} \times \\ &\quad \left[1 - \frac{\epsilon}{8} \frac{\zeta}{1+\zeta} \left\{ \frac{3}{2} - \frac{x+y}{4} + \frac{1-y}{x+y} \ln(1-y) - \right. \right. \\ &\quad \left. \left. \frac{1-y}{x+y} \ln(1+x) + \frac{1-x}{x+y} \ln(1-x) - \frac{1-x}{x+y} \times \right. \right. \\ &\quad \left. \left. \ln(1+y) + (f-2) \left[\frac{x+y}{4} - \frac{xy}{2(x+y)} - \frac{1}{x+y} \times \right. \right. \right. \\ &\quad \left. \left. \left. \ln(1+y) - \frac{1}{x+y} \ln(1+x) \right] \right\} \right] \quad (4.2) \end{aligned}$$

Therefore, the mean square radius of gyration is obtained from

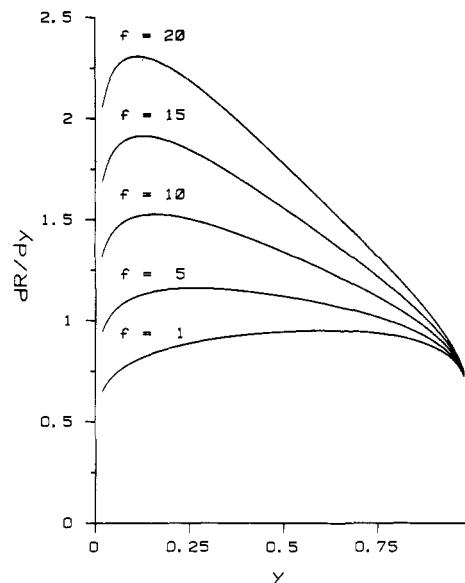


Figure 2. dR/dy vs. y in the self-avoiding limit for different values of f . $R = \langle r^2 \rangle_{0,y} / Nl(2\pi N/L)^{1/8}$ is the dimensionless mean square distance of a segment located at the contour distance Ny from the center of a star.

$$\begin{aligned} \langle S^2 \rangle &= \frac{1}{f} \int_0^1 dx \int_0^1 dy \langle r^2 \rangle_{x,y} + \\ &\quad \frac{f-1}{2f} \int_0^1 dx \int_0^1 dy \langle r^2 \rangle_{x,y'} = \frac{Ll}{2\pi} \left(\frac{2\pi N}{L} \right)^{2\nu(\zeta)} \left[\frac{3f-2}{6f} - \right. \\ &\quad \left. \frac{\epsilon}{8} \frac{\zeta}{\zeta+1} \left\{ \frac{13}{72} + \frac{(f-1)(3f-5)}{3f} \left(\frac{13}{12} - 2 \ln 2 \right) \right\} \right] \quad (4.3) \end{aligned}$$

Equation 4.3 reduces to the well-known Gaussian limit²⁴ involving the factor $(3f-2)/6f$. Again we recover the linear polymer limits²³ for $f=1$ or 2.

Figure ratio presents $R \equiv \langle r^2 \rangle_{0,y} / Nl(2\pi N/L)^{1/8}$ vs. y in the self-avoiding $\zeta = \infty$ limit. This gives the variation in the mean square distance of a segment from the center as a function of the contour length along a branch. (The normalization factor is just $\langle r^2 \rangle$ for the ends of a linear chain of length N in good solvents from the $\mathcal{O}(\epsilon)$ calculation.) Figure 2 provides the derivative with respect to y to indicate the substantial regions of linear dependence on y in contrast to bloblike assumptions even for $f=1$ or 2 of a linear dependence for small y , which becomes a $y^{2\nu}$ form for large y . Note that for large f we have instead a faster than linear rise, i.e., more expansion, for small y and a slower one for large y . Clearly, the simple blob-type models inadequately describe intersegment distances. RG calculations could be helpful in formulating better models, but then the RG analysis is now possible for interesting polymer quantities, so the blob model should be used with caution. As f increases, the local expansion about the star center increases, and the decreased expansion at the outer extremities continues. The former arises because of the higher density of segments near the star center. The expansion along the branch is surprisingly uniform for $f \leq 5$.

The ratio of $\langle S^2 \rangle_f$ to $\langle S^2 \rangle_{f=1}$ is presented as a function of the crossover parameter ζ for $\epsilon = 1$

$$\begin{aligned} S \equiv \langle S^2 \rangle_f / \langle S^2 \rangle_{f=1} &= \frac{3f-2}{f} \left[1 - \right. \\ &\quad \left. \frac{\epsilon}{8} \frac{\zeta}{1+\zeta} \left\{ \frac{13}{2} \frac{(f-1)(f-2)}{(3f-2)} - \frac{4(f-1)(3f-5)}{(3f-2)} \ln 2 \right\} \right] \quad (4.4) \end{aligned}$$

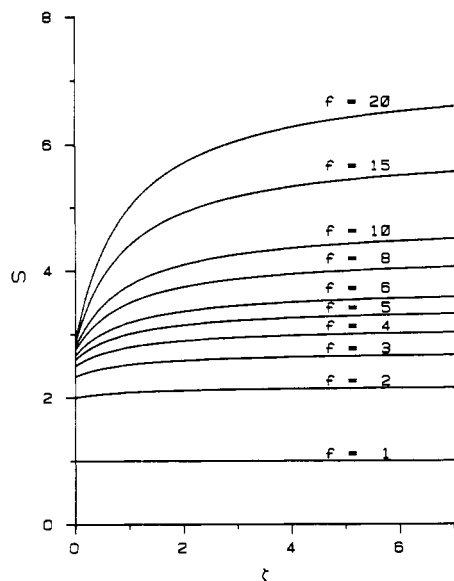


Figure 3. Relative mean square radius of gyration $S = \langle S^2 \rangle_f / \langle S^2 \rangle_{f=1}$ vs. the crossover parameter ζ for various values of number of branches f , where the length N of each branch is constant.

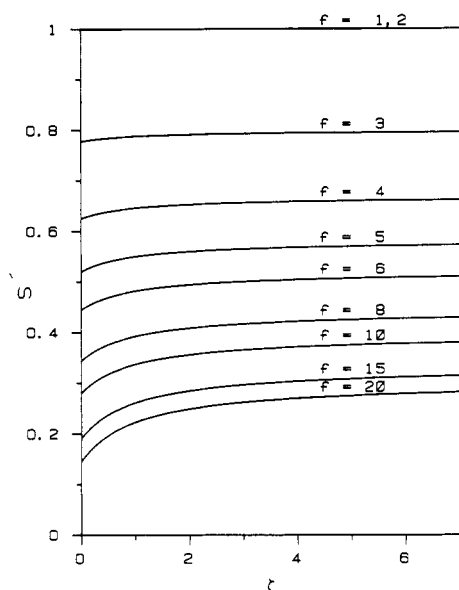


Figure 4. Relative mean square radius of gyration $S' = \langle S^2 \rangle'_f / \langle S^2 \rangle_{f=1}$ vs. the crossover parameter ζ for various values of f , where the total molecular weight of stars is kept constant, i.e., $fN = \text{constant}$.

in Figure 3 for a star polymer with f branches of length N . Polymer expansion with increased f is clear from Figure 3. If the overall molecular weight of the star is maintained constant, i.e., $fN = \text{constant}$, the ratio becomes

$$S' \equiv \langle S^2 \rangle'_f / \langle S^2 \rangle_{f=1} = \frac{3f-2}{f^2} \left[1 - \frac{\epsilon}{8} \frac{\zeta}{1+\zeta} \left\{ \frac{13}{2} \times \frac{(f-1)(f-2)}{(3f-2)} - \frac{4(f-1)(3f-5)}{(3f-2)} \ln 2 + \ln f \right\} \right] \quad (4.4')$$

and is also displayed in Figure 4, where the ratio for $f = 2$ is unity for any ζ , since this type of f dependence has often been considered in the literature.

V. Osmotic Second Virial Coefficient

The bare second virial coefficient for a star polymer with f branches of equal bare length N_0 and another with g

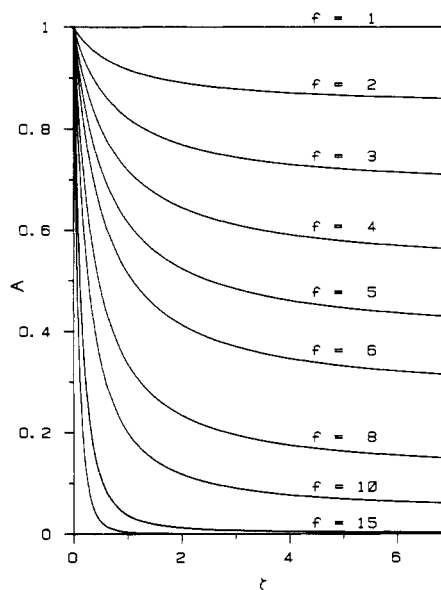


Figure 5. Relative osmotic second virial coefficient $A = A_2(f,N)/A_2(1,N)$ vs. the crossover parameter ζ for various values of number of branches f , where the length N of each branch is constant.

branches of equal bare length M_0 is defined by

$$A_{2B}(f, N_0; g, M_0) = - \frac{[P_2(f, N_0; g, M_0) - P_1(f, N_0)P_1(g, M_0)]N_A}{2VP_1(f, N_0)P_1(g, M_0)\mathcal{M}(fN_0)\mathcal{M}(gM_0)} \quad (5.1)$$

where P_2 and P_1 are the partition functions for the pair of interacting chains and for a single chain, respectively, N_A is Avogadro's number, V is the volume of the solution, and $\mathcal{M}(fN_0)$ is the molecular weight of the star polymer of f branches with length N_0 . The diagrams for calculating A_{2B} along with their values to order ϵ and v_0 are given in Appendix C.

The renormalized (self) second virial coefficient when $f = g$ and $N_0 = M_0$ is defined in the $a/L \rightarrow 0$ limit as

$$A_2(f, N; u, L) = A_{2B}(f, Z_2^{-1}N; u_0(u, a/L), a) = \frac{(l/d)^{d/2} u L^{-\epsilon/2} N_A (fN)^2}{2\mathcal{M}(fN)^2} (2\pi N/L)^{-(\epsilon/4)[\zeta/(1+\zeta)]} \times \left[1 - \frac{\epsilon}{8} \frac{\zeta}{1+\zeta} \{ 1 - 4 \ln 2 + (f-1)(16 \ln 2 - 9 \ln 3) + (f-1)^2(-14 \ln 2 + 9 \ln 3) \} \right] = \frac{\epsilon}{16} \frac{\zeta(1+\zeta)^{\epsilon/8} N_A f^2}{[1 + \zeta(1+\zeta)^{\epsilon/8}] \mathcal{M}(fN)^2} \left(\frac{Ll}{d} \right)^{d/2} (2\pi N/L)^{d\nu} \times \exp \left[- \frac{\epsilon}{8} \frac{\zeta}{1+\zeta} \{ 1 - 4 \ln 2 + (f-1) \times (16 \ln 2 - 9 \ln 3) + (f-1)^2(-14 \ln 2 + 9 \ln 3) \} \right] \quad (5.2)$$

where

$$d\nu = 2 - \frac{\epsilon}{2} + \frac{\epsilon}{4} \frac{\zeta}{1+\zeta} + \mathcal{O}(\epsilon^2) \quad (5.3)$$

(2.15), (3.12), and (3.14) are used to replace u , and the exponentiation is introduced to avoid obtaining unphysically negative values for A_2 when excluded volume is positive. The second virial coefficient is given previously¹⁹

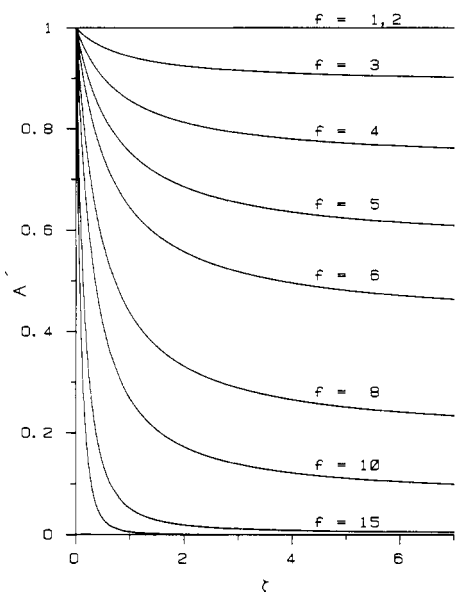


Figure 6. Relative osmotic second virial coefficient $A' = A'_2(f, N)/A_2(1, N)$ vs. the crossover parameter ζ for various values of f , where the total molecular weight is kept constant, i.e., $fN = \text{constant}$.

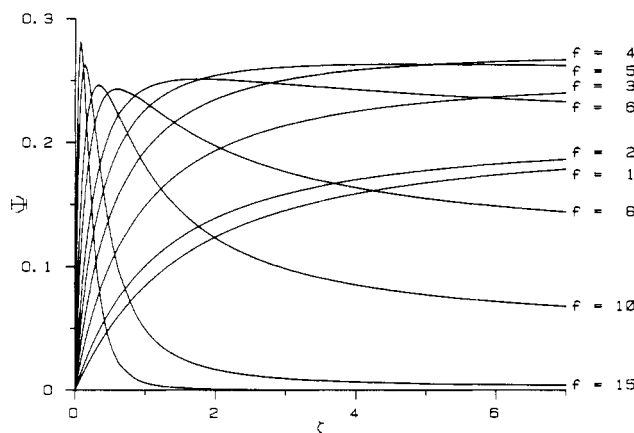


Figure 7. Interpenetration function Ψ vs. the crossover parameter ζ for various values of f , the number of branches. The curve with no f value is for $f = 20$.

for linear polymers $f = 1$ or 2 . Although the diagrams and renormalization are correctly presented, the final formula is incorrectly presented.²³

The ratio of $A_2(f, N)$ to $A_2(1, N)$ for fixed branch size N is obtained as

$$A \equiv A_2(f, N)/A_2(1, N) = \exp \left[-\frac{\epsilon}{8} \frac{\zeta}{1 + \zeta} \{ (f-1) \times (16 \ln 2 - 9 \ln 3) + (f-1)^2 (-14 \ln 2 + 9 \ln 3) \} \right] \quad (5.4)$$

and is depicted in Figure 5 as a function of ζ for $\epsilon = 1$. The effect of the branches is shown to become stronger as ζ increases. When the overall molecular weight of the star is kept constant, i.e., $Nf = \text{constant}$, utilizing the fact that u is independent of N and f , we obtain

$$A' \equiv A'_2(f, N)/A_2(1, N) = \exp \left[-\frac{\epsilon}{8} \frac{\zeta}{1 + \zeta} \{ (f-1)(16 \ln 2 - 9 \ln 3) + (f-1)^2 (-14 \ln 2 + 9 \ln 3) - 2 \ln f \} \right] \quad (5.4')$$

which is displayed in Figure 6, where the ratio for $f = 2$ is unity for any ζ . The decrease of A_2 in the self-avoiding limit is suppressed in Figure 6 in comparison with Figure 5.

The interpenetration function Ψ is defined in $d (=4 - \epsilon)$ dimensions by

$$\Psi = \frac{2A_2 \mathcal{M}(fN)^2 (d/3)^{d/2}}{(4\pi)^{d/2} \langle \mathbf{S}^2 \rangle^{d/2} N_A} \quad (5.5)$$

reducing to the conventional definition for $d = 3$.²⁵ Collecting the expressions for A_2 and $\langle \mathbf{S}^2 \rangle$ and exponentiating (4.3) also lead to

$$\Psi = \frac{\epsilon}{8} \frac{\zeta(1 + \zeta)^{\epsilon/8}}{1 + \zeta(1 + \zeta)^{\epsilon/8}} \left(\frac{f}{3f-2} \right)^{2-\epsilon/2} f^2 \exp \left[-\frac{\epsilon}{8} \frac{\zeta}{1 + \zeta} \times \left\{ 1 - 4 \ln 2 - \frac{13f}{6(3f-2)} + \frac{4(f-1)(3f-5)}{3f-2} \left(2 \ln 2 - \frac{13}{12} \right) + (f-1)(16 \ln 2 - 9 \ln 3) + (f-1)^2 (-14 \ln 2 + 9 \ln 3) \right\} \right] \quad (5.6)$$

which is independent of N apart from the implicit dependence of ζ on N . Ψ vs. ζ for $\epsilon = 1$ is presented in Figure 7. Here we notice that Ψ increases near the Gaussian limit of $\zeta \sim 0$, but it displays a maximum for $f = 4$ at the self-avoiding $\zeta = \infty$ limit.

VI. Discussion

The chain conformational space renormalization group method has been used to calculate the distribution functions for intersegment distance vectors, the mean square intersegment distances, the mean square radius of gyration, the osmotic second virial coefficient, and the interpenetration function for star polymers with f branches of equal lengths (i.e., branch molecular weights). Not only do the calculations provide the scaling functions and exponents ν , γ , etc., but we also consider all prefactors, numerical coefficients, etc., as well as the full crossover dependence on the strength of the excluded volume interaction and the chain length. The extension of the calculations to cases where the branches have unequal lengths or to other geometrical branching patterns like comb polymers is straightforward but too lengthy to present here.

The calculated results vividly exhibit how the local expansions near the center of the star polymer become more significant as f increases due to the higher segment density in that region. Furthermore, the local expansion is shown in Figure 2 to be diminished near the ends of the branches as if to compensate for the increased expansion in the interior of the star polymer. These features appear to be quite different from those proposed in the blob model by Daoud and Cotton,¹² who assumed the presence of three different regimes as a function of increasing distance from the center of the star: (1) the inner region is taken to be a close-packed core, (2) the intermediate region is argued to be Gaussian because of screening of excluded volume, and (3) the outer region has excluded volume effects within the blobs. Daoud has informed us of unpublished calculations showing increased stretching in the interior region, in agreement with our more rigorous theory.

Our polymer model (2.2) cannot be applied to the limit of rather large f where a central hard-packed core emerges, because this traditional δ function model in (2.2) is inadequate to describe hard-core packing. Recent experiments

by Huber et al.²⁶ suggest that these corrections are necessary for $f > 7$, so our theory is applicable for $f \lesssim 7$. We have extended the chain conformation space renormalization group theory to include three-body interactions which model the central hard-core packing in the θ -point region,²⁷ and it will be of interest to apply this theory to star polymers with large f . The model of Daoud and Cotton is probably more oriented to this high- f range. Their assumed intermediate-range screening is not observed in our calculations. Perhaps the fact that the branches are connected in a star leads to a qualitatively different type of "screening" than that due to separate chains in semidilute solutions.

In the crossover regime the polymer properties are dependent on a scaling variable ζ lying in the range $0 < \zeta < \infty$, with $\zeta \rightarrow 0$ giving the Gaussian chain limit and $\zeta \rightarrow \infty$ the self-avoiding chain limit of fully developed excluded volume. ζ is a renormalized version of the empirical z parameter of the two-parameter theory. ζ is proportional to $N^{1/2}$ (for $d = 3$) as well as a nonanalytic function of the renormalized, macroscopic excluded volume interaction. The latter is a complicated many-body quantity whose true dependence on the microscopic intersegment interaction is beyond the scope of the renormalization group theory. As emphasized previously¹⁹ the best comparison between experiment and theory is provided by considering a number of universal observables, which are functions of ζ only, and by eliminating ζ between them to provide relationships among different observables in the poorly understood and important crossover region. The use of star polymers with varying numbers f of branches or of comb, etc., polymers provides a wealth of this type of universal quantities. For instance, we have the ratios $\langle S^2 \rangle_f / \langle S^2 \rangle_{f=1}$ and $A_2(f, N) / A_2(1, N)$ for $f \geq 3$ as separate universal quantities. These considerations are important to test whether the simple model (2.2) is adequate to describe polymer properties in the crossover limit.

The calculated $\langle S^2 \rangle$ for constant N in Figure 3 is shown to be strongly dependent on f for $\zeta \gtrsim 1$ even though the effective exponent $\nu(\zeta)$ of (3.15) is identical with that for one of the branches alone ($f = 1$) as a linear polymer. This feature stresses the importance of calculating the prefactors and not just exponents as is done in scaling theories and in previous renormalization group methods. $\langle S^2 \rangle$ must reach a limiting value in real star polymers for $f \gg 1$, but, as already stressed above, this limit is outside the range of validity of the present model because of the lack of a hard core and because the Gaussian chain is infinitely extensible. Another exponent, describing the total partition function, $\gamma(\zeta)$, is strongly dependent on f , with its coefficient of $\epsilon = 4 - d$ vanishing for $f = 3$ and becoming negative for $f \geq 4$.

Traditional perturbation calculations²⁴ have already predicted a decrease in the second virial coefficient $A_2(f, N)$ with increasing f . However, the interpenetration function Ψ as a function of ζ emerges here with a more complicated dependence of f arising from the increase of $\langle S^2 \rangle$ with f and the decrease of A_2 with f , each with a different variation with ζ . Ψ for linear polymers, on the other hand, has been shown¹⁹ to be a monotonically increasing function of ζ . A_2 as evaluated in Appendix C has terms through order u^2 , but u is retained here only to order ϵ , thereby keeping only a portion of the ϵ^2 contributions. Recent second-order renormalization group calculations²⁸ have enabled us to determine the additional order ϵ^2 terms that increase A_2 for larger f and lead to a limiting $\zeta \rightarrow \infty$ value for Ψ which is slowly increasing with f in closer accord with expectations that Ψ approach a hard-sphere limit for large f . The results of this second-order calculation will be presented elsewhere.²⁹

Table I
Values of the Asymptotic $\zeta \rightarrow \infty$ Limiting Ψ^* for
Different Numbers of Branches f

f	Ψ^*	f	Ψ^*
1, 2	0.205 ^a	8	0.110
3	0.251	10	0.044
4	0.265	12	0.014
5	0.246	15	0.0015
6	0.205		

^a This value seems somewhat smaller than those reported elsewhere.²³

It should be noted that using the conventional $d = 3$ definition of Ψ

$$\Psi = A_2 M^2 / 4\pi^{3/2} \langle S^2 \rangle^{3/2} N_A \quad (6.1)$$

would lead to a calculated nonuniversal Ψ depending on N as

$$\Psi \sim (2\pi N/L)^{(\epsilon/16)[\zeta/(1+\zeta)]} \quad (6.2)$$

Since the present calculations use ϵ expansions, we emphasize that Ψ should be defined in the space of dimensionality $d = 4 - \epsilon$ as given by (5.5). This approach provides us with a Ψ that is a universal function of the scaling variable ζ . Note also that ζ is a function of N by (3.12). Hence, for the case in which we present results with $Nf = \text{constant}$ actually ζ has the f dependence of $f^{1/2}$. Values of the limiting $\zeta \rightarrow \infty$ universal, asymptotic limit Ψ^* of the penetration function are presented in Table I for various values of f .

The conformational space renormalization group method can likewise be applied to the calculation of other quantities that are related to thermodynamic and rheological properties of star polymers. These calculations are planned for future works in order to enable us to extract the scaling variable ζ from comparisons between theory and experiment. Recent renormalization group calculations for semidilute solutions of linear polymers show how ζ -dependent quantities at infinite dilution appear as fundamental scaling variables in the semidilute region.³⁰ A similar situation is anticipated for star polymers.

Acknowledgment. We are very grateful to Dr. Toshikazu Takada for his valuable help with computer work and also to Dr. Arkady Kholodenko for his comments on the manuscript. This research is supported, in part, by NSF Grant DMR 78-26630 (Polymers Program).

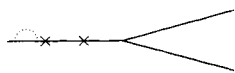
Appendix A. Intrabranched, Intersegment Distribution Function

The first-order contribution G_1 of (3.2) to $G_B(\mathbf{r}, x, y; v_0, N_0, a)$ has a number of contributions that are conveniently summarized diagrammatically. Each dotted line carries a $-v_0 \delta(\mathbf{r} - \mathbf{r}')$ factor, while the crosses (to be labeled x and y) represent the designated points with spatial separation $\mathbf{r} = (l/d)^{1/2} \mathbf{c}$. All other vertex points, junctions of dotted with solid lines, have integrations over their spatial and contour variables, and integrations are performed over the spatial positions of all branch end points. For instance, apart from a factor of $-v_0 N_0^2$ the diagram in (A.1) below has the value

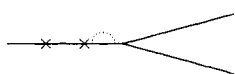
$$\prod_{j=2}^f \int d\mathbf{R}_j G_0(\mathbf{R}_j, N_0) \int d\mathbf{R}_1 \int d\mathbf{c}_1 \int d\mathbf{c}' \int_{y+a/N_0}^1 d\tau \int_y^{\tau-a/N_0} d\tau' G_0(\mathbf{R}_1 - \mathbf{c}', N_0(1-\tau)) G_0(0, N_0(\tau-\tau')) G_0(\mathbf{c}' - \mathbf{c}_2, N_0(\tau' - y)) G_0(\mathbf{c}, N_0(y-x)) G_0(\mathbf{c}_1, N_0 x)$$

When the spatial integrations are evaluated, the singularities in the τ and τ' integrals are extracted with the methods described previously¹⁸ involving introducing a cutoff a as a lower limit on any integrals that would otherwise be divergent. Then the integrals are expanded in ϵ through order ϵ^0 . The results of this procedure are summarized below and in the other appendices for each diagram individually to facilitate interested readers in checking their calculations by these methods. It should be noted that the present method provides final results for physical observables identical with those of dimensional regularization methods^{15,16,19} employed in some of the previous works on linear polymers.

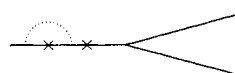
The contributions to $G_B(\mathbf{r}, x, y; v_0, N_0, a)$ of first order in v_0 and order ϵ^0 come from the following terms corresponding to each of the diagrams:



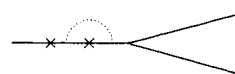
$$I_1 = \frac{N_0(1-y)}{a} - \ln \frac{N_0}{a} - \ln(1-y) - 1 \quad (\text{A.1})$$



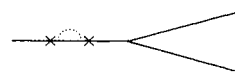
$$I_2 = \frac{N_0 x}{a} - \ln \frac{N_0}{a} - \ln x - 1 \quad (\text{A.2})$$



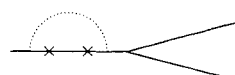
$$I_3 = \ln \frac{N_0}{a} + 2 + \frac{1}{\alpha_0} + \ln(y-x) - (\gamma + \ln \alpha_0) - \frac{1}{\alpha_0} \exp\left(-\alpha_0 \frac{y-x}{1-y}\right) - F\left(\alpha_0; \frac{1-y}{y-x}\right) \quad (\text{A.3})$$



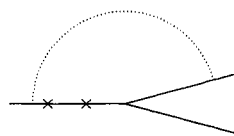
$$I_4 = \ln \frac{N_0}{a} + 2 + \frac{1}{\alpha_0} + \ln(y-x) - (\gamma + \ln \alpha_0) - \frac{1}{\alpha_0} \exp\left(-\alpha_0 \frac{y-x}{x}\right) - F\left(\alpha_0; \frac{x}{y-x}\right) \quad (\text{A.4})$$



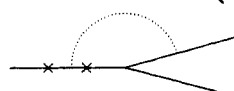
$$I_5 = \frac{N_0(y-x)}{a} - (\alpha_0 - 1) \ln \frac{N_0}{a} - 2 + (\alpha_0 - 1)[\gamma + \ln \alpha_0 - \ln(y-x) - 1] \quad (\text{A.5})$$



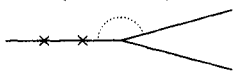
$$I_6 = E_1\left(\alpha_0 \frac{y-x}{x}\right) + E_1\left(\alpha_0 \frac{y-x}{1-y}\right) - E_1\left(\alpha_0 \frac{y-x}{1+x-y}\right) + \frac{1}{\alpha_0(y-x)} \left[(1+x-y) \exp\left(-\alpha_0 \frac{y-x}{1+x-y}\right) - x \exp\left(-\alpha_0 \frac{y-x}{x}\right) - (1-y) \exp\left(-\alpha_0 \frac{y-x}{1-y}\right) \right] \quad (\text{A.6})$$



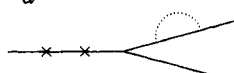
$$I_7 = E_1\left(\alpha_0 \frac{y-x}{1+x-y}\right) - E_1\left(\alpha_0 \frac{y-x}{2+x-y}\right) - E_1\left(\alpha_0 \frac{y-x}{x}\right) + E_1\left(\alpha_0 \frac{y-x}{1+x}\right) + \frac{1}{\alpha_0(y-z)} \left[(2+x-y) \exp\left(-\alpha_0 \frac{y-x}{2+x-y}\right) - (1+x-y) \exp\left(-\alpha_0 \frac{y-x}{1+x-y}\right) - (1+x) \exp\left(-\alpha_0 \frac{y-x}{1+x}\right) + x \exp\left(-\alpha_0 \frac{y-x}{x}\right) \right] \quad (\text{A.7})$$



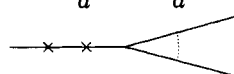
$$I_8 = \frac{1}{\alpha_0} \left[\exp\left(-\alpha_0 \frac{y-x}{x}\right) - \exp\left(-\alpha_0 \frac{y-x}{1+x}\right) \right] + F\left(\alpha_0; \frac{x}{y-x}\right) - F\left(\alpha_0; \frac{1+x}{y-x}\right) \quad (\text{A.8})$$



$$I_9 = \ln \frac{N_0}{a} + \ln x - \ln(1+x) + 1 \quad (\text{A.9})$$



$$I_{10} = \frac{N_0}{a} - \ln \frac{N_0}{a} - 1 \quad (\text{A.10})$$



$$I_{11} = \ln \frac{N_0}{a} + 1 - \ln 2 \quad (\text{A.11})$$


Here eq 3.5, 3.6, and 3.7 are used. The two branches to the right from the center in the diagrams stand for the other $f-1$ branches. G_1 of (3.2) is written in terms of the I_j as

$$G_1(\mathbf{c}, N_0 x, N_0 y) = G_0(\mathbf{c}, N_0(y-x)) \frac{1}{(2\pi)^2} [I_1 + I_2 + I_3 + I_4 + I_5 + I_6 + (f-1)(I_7 + I_8 + I_9 + I_{10}) + \frac{1}{2}(f-1)(f-2)I_{11}] \quad (\text{A.12})$$


providing us with (3.4).

Appendix B. Interbranch, Intersegment Distribution Function


For the calculation of $G_B'(\mathbf{r}, x, y; v_0, N_0, a)$, the contributions of the first order in v_0 are as follows:



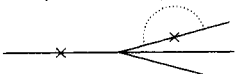
$$J_1 = \frac{N_0(1-y)}{a} - \ln \frac{N_0}{a} - \ln(1-y) - 1 \quad (\text{B.1})$$




$$J_2 = \frac{N_0(1-x)}{a} - \ln \frac{N_0}{a} - \ln(1-x) - 1 \quad (\text{B.2})$$




$$J_3 = \ln \frac{N_0}{a} + 2 + \ln(x+y) + \frac{1}{\alpha_0} - (\gamma + \ln \alpha_0) - \frac{1}{\alpha_0} \exp\left(-\alpha_0 \frac{x+y}{1-y}\right) - F\left(\alpha_0; \frac{1-y}{x+y}\right) \quad (\text{B.3})$$



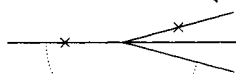
$$J_4 = \ln \frac{N_0}{a} + 2 + \ln(x+y) + \frac{1}{\alpha_0} - (\gamma + \ln \alpha_0) - \frac{1}{\alpha_0} \exp\left(-\alpha_0 \frac{x+y}{1-x}\right) - F\left(\alpha_0; \frac{1-x}{x+y}\right) \quad (\text{B.4})$$




$$J_5 = \frac{N_0(x+y)}{\alpha} - (\alpha_0 - 1) \ln \frac{N_0}{a} - 2 + (\alpha_0 - 1)[\gamma + \ln \alpha_0 - \ln(x+y) - 1] \quad (\text{B.5})$$



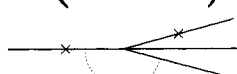
$$J_6 = E_1\left(\alpha_0 \frac{x+y}{1-x}\right) + E_1\left(\alpha_0 \frac{x+y}{1-y}\right) - E_1\left(\alpha_0 \frac{x+y}{2-x-y}\right) + \frac{1}{\alpha_0(x+y)} \left[(2-x-y) \exp\left(-\alpha_0 \frac{x+y}{2-x-y}\right) - (1-x) \exp\left(-\alpha_0 \frac{x+y}{1-x}\right) - (1-y) \exp\left(-\alpha_0 \frac{x+y}{1-y}\right) \right] \quad (\text{B.6})$$



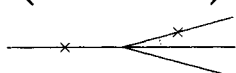
$$J_7 = \frac{1}{\alpha_0 y^2} \left[\{2(x+y) - y^2\} \exp\left(-\alpha_0 \frac{y^2}{2(x+y) - y^2}\right) - (x+y-y^2) \exp\left(-\alpha_0 \frac{y^2}{x+y-y^2}\right) - (x+y+xy) \exp\left(-\alpha_0 \frac{y^2}{x+y+xy}\right) \right] + \frac{x}{\alpha_0 y} \exp\left(-\alpha_0 \frac{y}{x}\right) - E_1\left(\frac{\alpha_0 y^2}{2(x+y) - y^2}\right) + E_1\left(\frac{\alpha_0 y^2}{x+y-y^2}\right) + E_1\left(\frac{\alpha_0 y^2}{x+y+xy}\right) - E_1\left(\frac{\alpha_0 y}{x}\right) \quad (\text{B.7})$$



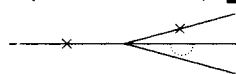
$$J_8 = \frac{1}{\alpha_0 x^2} \left[\{2(x+y) - x^2\} \exp\left(-\alpha_0 \frac{x^2}{2(x+y) - x^2}\right) - (x+y-x^2) \exp\left(-\alpha_0 \frac{x^2}{x+y-x^2}\right) - (x+y+xy) \exp\left(-\alpha_0 \frac{x^2}{x+y+xy}\right) \right] + \frac{y}{\alpha_0 x} \exp\left(-\alpha_0 \frac{x}{y}\right) - E_1\left(\frac{\alpha_0 x^2}{2(x+y) - x^2}\right) + E_1\left(\frac{\alpha_0 x^2}{x+y-x^2}\right) + E_1\left(\frac{\alpha_0 x^2}{x+y+xy}\right) - E_1\left(\frac{\alpha_0 x}{y}\right) \quad (\text{B.8})$$



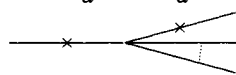
$$J_9 = \ln \frac{N_0}{a} + 2 + \frac{1}{\alpha_0} - (\gamma + \ln \alpha_0) + \ln(x+y) - E_1\left(\alpha_0 \frac{y}{x}\right) + \frac{1}{\alpha_0 y} \left[x \exp\left(-\alpha_0 \frac{y}{x}\right) - (x+y) \exp\left(-\alpha_0 \frac{y^2}{x+y+xy}\right) \right] - F'(\alpha_0; y) \quad (\text{B.9})$$



$$J_{10} = \ln \frac{N_0}{a} + 2 + \frac{1}{\alpha_0} - (\gamma + \ln \alpha_0) + \ln(x+y) - E_1\left(\alpha_0 \frac{x}{y}\right) + \frac{1}{\alpha_0 x} \left[y \exp\left(-\alpha_0 \frac{x}{y}\right) - (x+y) \exp\left(-\alpha_0 \frac{x^2}{x+y+xy}\right) \right] - F'(\alpha_0; x) \quad (\text{B.10})$$



$$J_{11} = \frac{N_0}{a} - \ln \frac{N_0}{a} - 1 \quad (\text{B.11})$$



$$J_{12} = \ln \frac{N_0}{a} - \ln 2 + 1 \quad (\text{B.12})$$

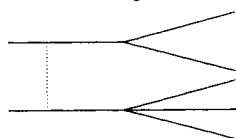
In deriving these results, we have used eq 3.5' and 3.7'. Here the two branches with no crosses to the right from the center in the diagrams stand for the other $f-2$ branches. G_1' is written in terms of the J_j as

$$G'(\mathbf{c}, N_0 x, N_0 y) = G_0(\mathbf{c}, N_0(x+y)) \frac{1}{(2\pi)^2} [J_1 + J_2 + J_3 + J_4 + J_5 + J_6 + (f-2)(J_7 + J_8 + J_9 + J_{10} + J_{11}) + \frac{1}{2}(f-2)(f-3)J_{12}] \quad (\text{B.13})$$

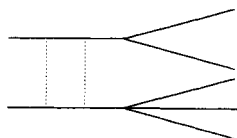
providing us with (3.4').

Appendix C. Osmotic Second Virial Coefficient

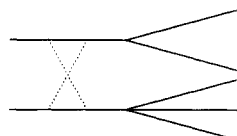
In order to calculate $A_{2B}(f, N_0, g, M_0)$ to order v_0^2 , we need to consider only the following contributions:



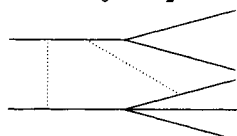
$$K_1 = -v_0 N_0 M_0 V \quad (\text{C.1})$$



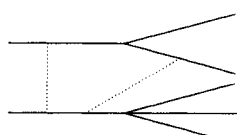
$$K_2 = \frac{v_0^2}{(2\pi)^2} N_0 M_0 V \left[-\ln a + \left(\frac{N_0}{2M_0} + 1 \right) \ln N_0 + \left(1 + \frac{M_0}{2N_0} \right) \ln M_0 - \frac{(N_0 + M_0)^2}{2N_0 M_0} \ln (N_0 + M_0) + \frac{1}{2} \right] \quad (C.2)$$



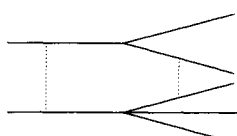
$$K_3 = K_2 \quad (C.3)$$



$$K_4 = \frac{v_0^2}{(2\pi)^2} N_0 M_0 V \left[2 \left(1 + \frac{M_0}{N_0} \right) \ln 2 + \frac{M_0}{N_0} \ln M_0 - \frac{N_0}{2M_0} \ln N_0 + \frac{(N_0 + M_0)^2}{N_0 M_0} \ln (N_0 + M_0) - \frac{(N_0 + 2M_0)^2}{2N_0 M_0} \ln (N_0 + 2M_0) \right] \quad (C.4)$$



$$K_5 = \frac{v_0^2}{(2\pi)^2} N_0 M_0 V \left[2 \left(\frac{N_0}{M_0} + 1 \right) \ln 2 + \frac{N_0}{M_0} \ln N_0 - \frac{M_0}{2N_0} \ln M_0 + \frac{(N_0 + M_0)^2}{N_0 M_0} \ln (N_0 + M_0) - \frac{(2N_0 + M_0)^2}{2N_0 M_0} \ln (2N_0 + M_0) \right] \quad (C.5)$$



$$K_6 = \frac{v_0^2}{(2\pi)^2} N_0 M_0 V \left[-2 \ln 2 \left\{ \frac{(N_0 + M_0)^2}{N_0 M_0} + \frac{N_0}{M_0} + \frac{M_0}{N_0} \right\} - 4 \frac{(N_0 + M_0)^2}{N_0 M_0} \ln (N_0 + M_0) + \frac{(2N_0 + M_0)^2}{N_0 M_0} \ln (2N_0 + M_0) + \frac{(N_0 + 2M_0)^2}{N_0 M_0} \ln (N_0 + 2M_0) - \frac{N_0}{M_0} \ln N_0 - \frac{M_0}{N_0} \ln M_0 \right] \quad (C.6)$$

Each diagram shows excluded volume interactions between a star polymer of f branches with equal length N_0 (upper) and another star polymer of g branches with equal length M_0 . Taking account of (2.1), we have

$$A_{2B}(f, N_0; g, M_0) = - \frac{N_A (l/d)^{d/2}}{2V \mathcal{M}(fN_0) \mathcal{M}(gM_0)} [fg(K_1 + K_2 + K_3) + fg(g-1)K_4 + f(f-1)gK_5 + \frac{1}{2}f(f-1)g(g-1)K_6] \quad (C.7)$$

which leads to

$$A_{2B}(f, N_0; g, M_0) = \frac{(l/d)^{d/2} v_0 N_A (fN_0)(gM_0)}{2\mathcal{M}(fN_0) \mathcal{M}(gM_0)} \left[1 - \frac{v_0}{(2\pi)^2} \left\{ -2 \ln a + \left(\frac{N_0}{M_0} + 2 \right) \ln N_0 + \left(2 + \frac{M_0}{N_0} \right) \ln M_0 - \frac{(N_0 + M_0)^2}{N_0 M_0} \ln (N_0 + M_0) + 1 + (f-1) \left[2 \left(\frac{N_0}{M_0} + 1 \right) \ln 2 + \frac{N_0}{M_0} \ln N_0 - \frac{M_0}{2N_0} \ln M_0 + \frac{(N_0 + M_0)^2}{N_0 M_0} \ln (N_0 + M_0) - \frac{(2N_0 + M_0)^2}{2N_0 M_0} \ln (2N_0 + M_0) \right] + (g-1) \left[2 \left(\frac{M_0}{N_0} + 1 \right) \ln 2 + \frac{M_0}{N_0} \ln M_0 - \frac{N_0}{2M_0} \ln N_0 + \frac{(N_0 + M_0)^2}{N_0 M_0} \ln (N_0 + M_0) + M_0 - \frac{(N_0 + 2M_0)^2}{2N_0 M_0} \ln (N_0 + 2M_0) \right] + \frac{1}{2}(f-1)(g-1) \left[-4 \left(1 + \frac{N_0}{M_0} + \frac{M_0}{N_0} \right) \ln 2 - 4 \frac{(N_0 + M_0)^2}{N_0 M_0} \ln (N_0 + M_0) + \frac{(2N_0 + M_0)^2}{N_0 M_0} \ln (2N_0 + M_0) + \frac{(N_0 + 2M_0)^2}{N_0 M_0} \ln (N_0 + 2M_0) - \frac{N_0}{M_0} \ln N_0 - \frac{M_0}{N_0} \ln M_0 \right] \right\} \right] \quad (C.8)$$

Putting $f = g$ and $N_0 = M_0$, we obtain $A_{2B}(f, N_0, u_0, a)$ from (C.8).

References and Notes

- (1) Zilliox, G. J. *Makromol. Chem.* **1972**, *156*, 121.
- (2) Toporowski, P. M.; Roovers, J. E. *Macromolecules* **1978**, *11*, 365.
- (3) Bauer, B. J.; Hadjichristidis, N.; Fetters, L. J.; Roovers, J. E. *J. Am. Chem. Soc.* **1980**, *102*, 2410.
- (4) Roovers, J. E.; Bywater, S. *Macromolecules* **1972**, *5*, 385; **1974**, *7*, 443.
- (5) Bywater, S. *Adv. Polym. Sci.* **1979**, *30*, 90.
- (6) Meerwall, E.; Tomich, D. H.; Hadjichristidis, N.; Fetters, L. J. *Macromolecules* **1982**, *15*, 1157.
- (7) Casassa, E. F.; Berry, G. C. *J. Polym. Sci., Part A-2* **1966**, *4*, 881.
- (8) Burchard, W. *Macromolecules* **1974**, *7*, 835.
- (9) Mattice, W. L. *Macromolecules* **1977**, *10*, 1171; **1981**, *14*, 143.
- (10) Mansfield, M. L.; Stockmayer, W. H. *Macromolecules* **1980**, *13*, 1713.
- (11) Pearson, D. S.; Raju, V. R. *Macromolecules* **1982**, *15*, 294.
- (12) Daoud, M.; Cotton, J. P. *J. Phys. (Paris)* **1982**, *43*, 531.
- (13) de Gennes, P.-G. "Scaling Concepts in Polymer Physics"; Cornell University Press: Ithaca, NY, 1979.
- (14) Daoud, M.; Cotton, J. P.; Farnoux, B.; Jannink, G.; Sarma, G.; Benoit, H.; Picot, C.; Duplessix, R.; de Gennes, P.-G. *Macromolecules* **1975**, *8*, 804.
- (15) Oono, Y.; Ohta, T.; Freed, K. F. *J. Chem. Phys.* **1981**, *74*, 6458.
- (16) Lipkin, M.; Oono, Y.; Freed, K. F. *Macromolecules* **1981**, *14*, 1270.
- (17) Oono, Y.; Ohta, T. *Phys. Lett. A* **1981**, *85*, 480.

- (18) Ohta, T.; Oono, Y.; Freed, K. F. *Phys. Rev. A* **1982**, *25*, 2801.
 (19) Oono, Y.; Freed, K. F. *J. Phys. A* **1982**, *15*, 1931.
 (20) For a review, see: Freed, K. F. *Adv. Chem. Phys.* **1972**, *22*, 1.
 (21) Amit, D. J. "Field Theory, The Renormalization Group and Critical Phenomena"; McGraw-Hill: New York, 1978.
 (22) National Bureau of Standards, "Handbook of Mathematical Functions with Formulas, Graphs, and Mathematical Tables"; Appl. Math. Ser. 55, 1972, p 228.
 (23) Oono, Y.; Kohmoto, M., to be published in *J. Chem. Phys.*
 (24) Zimm, B. H.; Stockmayer, W. H. *J. Chem. Phys.* **1949**, *17*, 1301.
 (25) Yamakawa, H. "Modern Theory of Polymer Solutions"; Harper & Row: New York, 1971; p 168.
 (26) Huber, K.; Burchard, W.; Fetters, L. J., preprint.
 (27) Kholodenko, A. L.; Freed, K. F., to be published.
 (28) Kholodenko, A. L.; Freed, K. F. *J. Chem. Phys.*, in press.
 (29) Douglas, J.; Freed, K. F., to be published.
 (30) Freed, K. F. *J. Chem. Phys.*, in press.

Notes

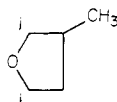
¹³C NMR Spectroscopic Study of the Microstructure of Poly(3-methyltetrahydrofuran)

LEONCIO GARRIDO, JULIO GUZMÁN,* and
 EVARISTO RIANDE

*Instituto de Plásticos y Caucho, Madrid 6, Spain.
 Received June 8, 1982*

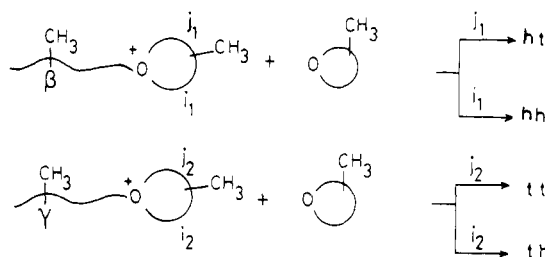
From thermodynamic considerations it was concluded in the past that substituted tetrahydrofuran could not polymerize due to the fact that substitution of hydrogen atoms by methyl groups in heterocyclic compounds render the free energy of polymerization positive.¹ However, Chiang and Rhodes² accomplished the polymerization of 3-methyltetrahydrofuran at several temperatures. The polymers obtained were of low molecular weight because transfer reactions probably took place during the polymerization process. More recently, the kinetic and thermodynamic aspects of the cationic polymerization of 3-methyltetrahydrofuran were studied at temperatures lying in the range 0 to -12 °C using an initiator with a very stable counterion: acetyl hexafluoroantimonate.³ With this catalyst, "living polymers" were obtained. On the other hand, it was found that the ceiling temperature of 3-methyltetrahydrofuran is 4 ± 1 °C, a value significantly lower than that reported for the polymerization of tetrahydrofuran (THF), which is in the vicinity of 86 °C.⁴ The enthalpy and entropy of polymerization also were calculated and their values were -5.4 kcal mol⁻¹ and -19.5 cal K⁻¹ mol⁻¹, respectively.³ The former value is similar to that obtained for THF, but the latter is lower than that found for the entropy of bulk polymerization of THF (-12.5 cal K⁻¹ mol⁻¹)⁴⁻⁹.

3-Methyltetrahydrofuran presents two different adjacent carbon atoms to the monomeric oxygen atom; as a consequence, the ring opening of the heterocycle can occur at *i* or *j* bonds in the monomer ring



and therefore different structures may be formed. In this work we report preliminary results on the microstructure of poly(3-methyltetrahydrofuran), as determined by ¹³C NMR spectroscopy.

Scheme I



Experimental Part

Materials. The monomer (3-methyltetrahydrofuran) (Fluka), acetyl chloride (Merck), and silver hexafluoroantimonate (Ventron) were purified as previously described.³ The initiator acetyl hexafluoroantimonate was prepared according to procedures described elsewhere.³

Polymerization. Bulk polymerizations of the monomer were carried out under high vacuum at -4 °C (polymer A) and -25 °C (polymer B) using initiator concentrations of 2.6×10^{-2} and 0.85×10^{-2} mol L⁻¹, respectively. The polymerization reactions were terminated with an aqueous solution of sodium carbonate, and the polymers were extracted with benzene, precipitated with methanol, and, finally, freeze-dried from benzene solutions at room temperature. The values of the number-average molecular weight of the polymers, determined at 37 °C in chloroform solutions with a Knauer vapor pressure osmometer, are shown in Table II.

¹³C NMR Analysis. The ¹³C NMR spectra of the polymers were recorded at 26 °C with a Bruker HX-90E Fourier transform spectrometer at 22.63 MHz, using deuterated chloroform as solvent and tetramethylsilane as internal reference. Quantitative spectra were obtained by using long pulse delay times (>10 s) and inverse gated decoupling techniques in order to eliminate the nuclear Overhauser enhancement.

Results and Discussion

In a recent work³ it was reported that the mechanism of the cationic polymerization of 3-methyltetrahydrofuran is similar to that of tetrahydrofuran. The polymerization reaction is produced by nucleophilic attack of the monomer oxygen atom on the carbon atom in α position relative to the oxonium ions, according to the mechanism shown in Scheme I, where hh, ht, th, and tt refer, respectively, to head-to-head, head-to-tail, tail-to-head, and tail-to-tail structures. As in the case of poly(2-methyloxacyclobutane), the fraction of the different structures along the chains can be quantitatively estimated by ¹³C NMR spectroscopy.^{10,11} The ¹³C NMR spectrum of the polymer, shown in Figure